A solar powered off-grid air conditioning system with natural refrigerant for residential buildings: A theoretical and experimental evaluation

Cleaner Energy Systems 5 (2023) 100077

Contents lists available at ScienceDirect

Cleaner Energy Systems

journal homepage: www.elsevier.com/locate/cles

A solar powered off-grid air conditioning system with natural refrigerant for residential buildings: A theoretical and experimental evaluation

Adam Y. Sulaiman [a,*], Gerard I. Obasi [a], Roma Chang [a], Hussein Sayed Moghaieb [b], Jayanta D. Mondol [a], Mervyn Smyth [a], Babak Kamkari [a], Neil J. Hewitt [a]

[a] Centre for Sustainable Technologies, Ulster University, Belfast, BT15 1ED, UK
[b] Nanotechnology and Integrated Bioengineering Centre, Ulster University, Belfast, BT15 1ED, UK

ARTICLE INFO

Keywords:
Natural refrigerants
GWP
Air-conditioning
PV panel
Energy storage
Exergy

ABSTRACT

Residential air-conditioning units are essential for providing suitable interior comfort in regions experiencing hot climates. Nonetheless, these units contribute significantly to CO_2 emissions in these countries due to their reliance on non-renewable energy sources and the use of environmentally unfriendly working fluids. This research aims to evaluate the feasibility of operating an off-grid solar-powered air-conditioning bed unit using low-GWP refrigerants that can efficiently replace conventional refrigerants. A model was developed to evaluate the vapour compression cycle's energetic and exergetic performance. Various refrigerants were employed as feeds to the mathematical model in order to simulate the unit's performance if environmentally friendly refrigerants supersede the conventional substances. An assembled prototype air-conditioning unit was built to provide cold air to a connected canopy. Two 400 W photovoltaic panels power this system, with battery storage providing electricity to the unit at night. TRNSYS was used to evaluate the batteries' energy storage capability, whilst Integrated Environmental Solutions Virtual Environment (IESVE) was used to estimate the amount of solar energy required to power the unit. On the basis of the energetic and exergetic findings, R290 and R600a have demonstrated their suitability as replacements for conventional refrigerants. In comparison to R134a, the system showed a 2.42% improvement in COP when using R290. This improvement was accompanied by a reduction in input work by 2.31% and an increase in exergetic efficiency by 2.37%. This paper provides a guideline for analytical design, combined with a coherent process system. This offers an excellent solution to the very real problems of major energy consumption in warm countries, combining a renewable energy source with an eco-friendly air-conditioning cycle.

1. Introduction

Greenhouse gas (GHG) emissions have doubled between 1970 and 2010 and their atmospheric concentrations have increased to the highest level by 1990 (Brückner et al., 2015), which led to a noticeable change in the earth's climate over the last decades. The excessive utilisation of fossil fuels is a primary factor raising the atmospheric concentration of CO_2 by 31%, and the atmospheric concentration of CH_4 by 151% between 1750 to 2000 (Ianc et al., 2020). In 2017, global warming reached 1 °C above the pre-industrial level and increased by 0.87 °C between 2006 and 2015 (Allen et al., 2019). According to the intergovernmental panel on climate change (IPCC), the earth is projected to have an increase in surface temperature by the end of the 21st century (Van Vuuren et al., 2008). According to (Chen, 2021), the global atmospheric CO_2 concentration rose to 415 ppm in 2020 from 285 ppm in 1850, leading to a 1.2 °C increase in the global average surface temperature. Reducing GHG emissions globally in 2050 will increase the chance of keeping the warming below 1.5 °C. This would require at least a 45% reduction from the 2010 level in 2030 in order to reach net-zero CO_2 emissions by 2050 (O'Neill et al., 2017). Global decarbonisation would demand different actions including the reduction of energy demand, decarbonisation of the electricity sector, and the electrifying of the industrial sector that utilises fossil fuels. To maintain the global temperature below 2 °C by 2100 (Agreement, 2015), the Paris Agreement designed a framework to pursue developing countries in their climate mitigation and specifically increased efforts to maintain the temperature below 1.5 °C because the slight increase between 1.5 °C and 2 °C could have a massive adverse impact on low-lying countries. To achieve this goal, conventional miti-

* Corresponding author.
E-mail address: sulaiman-w@ulster.ac.uk (A.Y. Sulaiman).

https://doi.org/10.1016/j.cles.2023.100077
Received 14 June 2022; Received in revised form 2 June 2023; Accepted 3 June 2023
Available online 4 June 2023

Nomenclature

A	area of the enclosed canopy (m^2)
B_c	battery capacity (W-hr.)
c_p	specific heat (kJ/kg.K)
COP	coefficient of performance (-)
D_c	daily electricity consumption (kW)
E	the rate of exergy output (kW)
e_{qc}	open circuit voltage at full charge
Ex	exergy destruction (kW)
F	fractional state of charge
g_c, g_d	small-valued coefficient of (1-F)
h	specific enthalpy (kJ/kg)
I	current (A)
k	Thermal conductivity (W/m-k)
$\dot{m}$	air mass flow rate of air (kg/s)
m_c, m_d	cell–type parameter
P	power (kW)
q	heat transfer rate (W)
Q_m	rated capacity of a cell
r_{qc}	internal resistance at full charge
RE	specific refrigerant effect (kJ/kg)
R_t	AC unit running time (hr)
T	temperature (°C)
t	thickness of canopy material (m)
ΔT	temperature difference (°C)
V	voltage (volt)
$\dot{V}$	air volume flow rate (m^3/s)
VHC	volumetric heat capacity (kJ/m^3)
$\dot{w}$	compressor's specific work (kJ/kg)

Greek symbols

η	Efficiency (%)
ρ	supplied air density (kg/m^3)
0	reference state point

Abbreviations

AC	air conditioning
CFC	chlorofluorocarbon
EES	engineering equation solver
GHG	greenhouse gas
GWP	global warming potential
HCFO	Hydrochlorofluoroolefins
HFC	hydrofluorocarbon
IPCC	intergovernmental panel on climate change
ODP	ozone depletion potential
VCC	vapor compression cycle

Subscripts

act	actual
ave	average
cd	conduction
comp	compressor
cond	condenser
cr	critical
dest	destruction
evap	evaporator
evap	evaporator
ex	exergetic
in	inlet
ise	isentropic
occ	occupants
out	outlet
sa	supplied air
th	theoretical
tot	total
vol	volumetric

gation technologies are being used to decrease CO_2 emissions from fossil fuels (Fawzy et al., 2020).

In developing countries and during the summer, the combination of high ambient temperatures and poor building architecture, dramatically increases interior rooms temperature. Overheating of the indoor and outdoor temperature has adverse effects on thermal comfort, health of the people, electricity consumption for cooling, peak energy demand, and the worldwide and local economies (Santamouris, 2015). In June of 2022, the Middle East, North Africa, Europe, and Asia were afflicted by heatwaves, with temperatures exceeding 40 °C and breaking the records that had been in place for a long time (Nasa, 2022). In addition to an increase in the intensity and frequency of heatwaves, as well as rising temperatures averaging, there is a growing demand for space cooling via the use of air conditioning to mitigate the heatwave's negative effects on both health and comfort (Viguié et al., 2020). Commonly accepted techniques for preventing overheating in built environments include using air conditioning systems to cool indoor spaces and mitigating the effects of outdoor heat (Santamouris and Feng, 2018). Rising demand for cooling in the future will result in higher energy consumption, leading to increased greenhouse gas emissions. This will also create considerable pressure on electricity grids globally as they struggle to cope with the surge in peak demand (EIA, 2021).

According to a report released by the International Energy Agency (IEA, 2018), the cooling of buildings contributes to about 20% of the global electricity consumption, and it is anticipated that by 2050, the amount of electricity used for cooling will more than triple. Due to the expansion of urban areas, increased access to electricity, higher incomes, and declining prices of air conditioners in many developing nations, the global market for room air conditioners is expanding rapidly. According to survey conducted by (JRAIA, 2022), the total number of duct-less room air conditioners installed worldwide in 2021 was 95,162, an increase of approximately 1.3% from the previous year. If current trends persist, there will be a significant increase in the global stock of mini-split air conditioners by 2030 and 2050. Specifically, the number of units is projected to rise by 1.21 billion and 3.28 billion, respectively, compared to 2015 levels. By 2050, demand for mini-split air conditioning is expected to be 3.75 times higher than in 2015, with implications for electricity generation and peak demand, especially in countries with hot climates. Additionally, this expansion is predicted to contribute significantly to greenhouse gas emissions (IEA, 2018).

The necessity of utilising AC units is contradicting the operational cost, leaving many lower-income families are unable to afford to cool their homes, particularly in regions with poor infrastructures, such as the Middle East, North Africa, and South America. When a population group operates a large number of AC units simultaneously, the energy demand overloads the electrical grid, resulting in a potential power supply failure (Allamraju and Characterization, 2013). To address both the high cost associated with high electric energy consumption and the negative impacts associated with burning fossil fuels to generate this electric energy, reliance on renewable energy is the optimal choice. Solar energy is one of the renewable energy sources that are a promising alternative to fossil fuels. Solar energy systems are expected to supply approximately 70% of the world's total energy consumption by 2100 as a result of technological advancements, ongoing scientific research, and positive government support (Clerici and Alimonti, 2015). With such abundant solar energy available, the challenge is to harness and convert it into usable forms of energy via cost-effective, efficient, and environmentally friendly energy conversion systems (Clerici and Alimonti, 2015).

To identify the knowledge gaps related to the present research, it was essential to review the most recent solar-powered air conditioning research activities. Chua et al. (2013) has conducted a comprehen-

sive literature review and critical assessment of the inherent benefits of cutting-edge cooling technologies and energy-saving strategies. Several renewable energy-assisted air conditioners, including absorption, adsorption, and mechanically driven vapour compression systems, were described in the article. In warm, hot countries, solar energy is an effective heat source for operating these cooling systems, according to the research. By employing novel technologies and strategies, the energy expenses associated with running air conditioning systems can be curtailed, thereby minimising the harmful impact on the environment and reducing the electricity costs needed to ensure thermal comfort in developing countries.

An investigation was conducted into a novel solar-powered air conditioner consisting of a hybrid air conditioner and a hybrid solar collector (Al-Alili et al., 2012). The TRNSYS simulation programme was employed to simulate the transient charging and discharging of batteries. The findings of the modelling study indicate that the area of the concentrating photovoltaic/thermal collector is the most influential factor on the system's performance. The results also indicated that integrating a desiccant wheel cycle with a conventional VCC is more effective than the standalone VCC in ensuring building comfort in humid and hot environments. In addition, the simulation revealed that the hybrid solar air conditioner has a higher COP than a VCC powered by PV panels and a solar absorption cycle. The study showed that the typical cooling COPs are 0.68, 0.34, and 0.29, respectively. In addition, Fong et al. (2011) analysed the feasibility of incorporating a solar-powered ejector into a solar-electric refrigeration system. The conclusion of the study was that the annual energy performance of the system could be improved by incorporating the ejector. The system with and without an ejector when using the refrigerants R22, R134a, and R410A was compared and evaluated using dynamic simulation. Compared to the other candidates, the system employing R134a demonstrated the greatest energy efficiency, as determined by the research.

Further study conducted by Eveloy Valerie and Yusra Alkendi. (2021) investigated the effectiveness of a space cooling system driven by low-grade solar thermal energy that utilizes compression-assisted, multi-ejector technology for a 36-kW air conditioning application. The study evaluated the performance of the system with four different working fluids: R11, R141b, R245fa, and R600a. The results showed that the ejector assembly was the main source of exergy destruction, but its efficiency improved with compression rose. The system has the potential to reduce annual electricity consumption for cooling by more than 40% compared to traditional split air conditioners, which can lead to significant cost savings and a reduction in greenhouse gas emissions. Additionally, Ghodbane et al. (2021) conducted a study evaluating a solar-powered ejector air conditioning system to accommodate the warm climate of southern Algeria. The investigation used water (R718) as the working fluid and a dynamic model to simulate a 12.5 kW cooling load unit. Furthermore, Al-Yasiri et al. (2022) carried out an in-depth assessment of solar-powered cooling and air-conditioning systems for building applications. The study encompassed the most recent findings concerning vapour compression, absorption, and adsorption air conditioning systems. The primary approach of operation for each type is described in this literature, and recent advancements are highlighted.

Based on the review of relevant literature, it is evident that prior research has primarily investigated the absorption and adsorption of cooling systems powered by solar panels. However, there is a substantial knowledge gap regarding the integration of mini-split vapour compression air conditioning units with solar panels. To address this gap, the current study proposes an innovative solution: the development and assessment of a solar-powered mini-split air conditioning bed unit. This system has enormous potential for serving low-income households in developing countries, as it requires considerably less input power. This system offers a more energy-efficient alternative to conventional split units by cooling a canopy at night. In addition, the paper examines the essential aspect of transitioning to natural refrigerants, specifically R290 as a potential drop-in substitution to conventional refrigerants. This investigation is in line with the rising global demand for environmentally favourable air conditioning technologies. Overall, this research addresses a notable research gap, offers an innovative solution with the potential for significant social impact, and contributes to ongoing efforts to develop sustainable air conditioning technologies.

2. Refrigerants under consideration

The outright bans and phase-down of HFCs on the market and restrictions on maintenance of equipment using HFCs are the main features of the fluorinated GHG (F-Gas) regulations. Reducing the F-Gas emissions by two-thirds of 2010 by 2030 and replacing that using environmentally friendly alternatives is the main goal of the F-Gas regulations (van Soest et al., 2017). Another serious issue with AC systems is the adverse effects of using conventional refrigerants as the working medium. Residential AC systems are thought to consume the most hydrofluorocarbon (HFC) and thus contribute significantly to GHG emissions, owing to the large number of units sold in warm- and hot-climate countries. For instance, the United States emitted 36.7 million metric tons of carbon dioxide in 2014, accounting for approximately 22% of total national HFC emissions due to the use of residential air conditioning units (Isaifan and Baldauf, 2020). Refrigerants with high GWP contribute significantly to GHG emissions, which is one of the primary causes of global warming, specifically when they escape to the atmosphere during operation or maintenance (98/04207 An experimental evaluation of the greenhouse effect in R22 substitution, 1998).

In the past few decades, hydrochlorofluorocarbons (HCFCs), such as R22, and HFCs, such as R134a, were the most common refrigerants used in AC systems and heat pumps due to their favourable thermodynamic characteristics (Johnson, 1998). However, developing countries are required to phase out HFCs and HCFCs by 2010 and 2040, respectively. In addition, the Kyoto Protocol, in 1997, imposed additional restrictions on the use of conventional refrigerants due to their GWP value, with the goal of mitigating climate change. F-Gas regulations targeted substances that can be released into the atmosphere by ACs, heat pumps, refrigeration systems, and ORCs, such as R22, R134a, and R410A (F-Gas Regulations). R32, which is the focus of this study, maybe a viable alternative to the conventional refrigerants used in residential air conditioning units. It also has no ozone layer depletion (ODP) value and a GWP of 677, which is less than the 750 limits for F-gas regulation. Even though R32 is classified as flammable gas, it is difficult to ignite due to its low value of lower flammable limits (Mota-Babiloni et al., 2017). In addition, R32 is gaining momentum due to its similarity of thermal properties and a COP value closer to R410A across various ranges of operating temperatures. Furthermore, it has a higher heat transfer coefficient value due to its higher liquid thermal conductivity which enables the AC system to cope with lower condensing temperatures (Pham and Rajendran, 2012). Moreover, R32 has a relatively lower mass flow rate leading to lower pressure drops among the AC system. The cost of R32 per kg is relatively lower than that of R410 and R22 (Pham and Rajendran, 2012). The refrigerant also offers a better COP value at higher ambient conditions, similar system pressure and pressure ratio which can be an alternative to R410 without major system redesign. One more advantage is that R32 has a lower system charge requirement due to it is lower system density value (Xu et al., 2013). Regardless of having zero ODP and neglected value of GWP, Propane (R290) has a similar capacity and pressure level of R22 and thus, R290 can replace R22. The non-toxic with very low GWP and zero-ODP Isobutane (R600a) can be also an alternative substitution for R134a in small AC units (Urchueguía et al., 2004). Several theoretical and experimental studies analysed and evaluated HCs performance for comprehensive heating, ventilation, and air conditioning (HVAC) application. The literature reveals that using R290 to replace R22 in a commercial refrigeration unit can increase the COP of the unit by 1-3% and a 13-20% decrease in capacity (El-Morsi, 2015). The energetic and exergetic performance studies of R290, R600a, and R134a were conducted, as the results showed that R600a has the high-

Table 1
The properties of the investigated refrigerants (ASHRAE, 2020; Lemmon et al., 2010).

Refrigerant	Formula	ODP	GWP/100yrs	$Safety_{des}$	T_{Cr} (°C)	Molar mass (g/mol)	P_{Cr} (bar)
R32	CH_2F_2	0	543	A_2	78.11	52.024	57.82
R410A	R32/R125	0	2000	A_1/A_1	71.35	72.585	49.02
R134a	CF_3CH_2F	0	1320	A_1	101.06	102.03	40.59
R22	$CHClF_2$	0.05	1780	A_1	96.2	86.468	49.9
R290	C_3H_8	0	3	A_3	96.7	44.097	42.5
R600a	C_4H_{10}	0	3	A_3	135	58.12	52.9

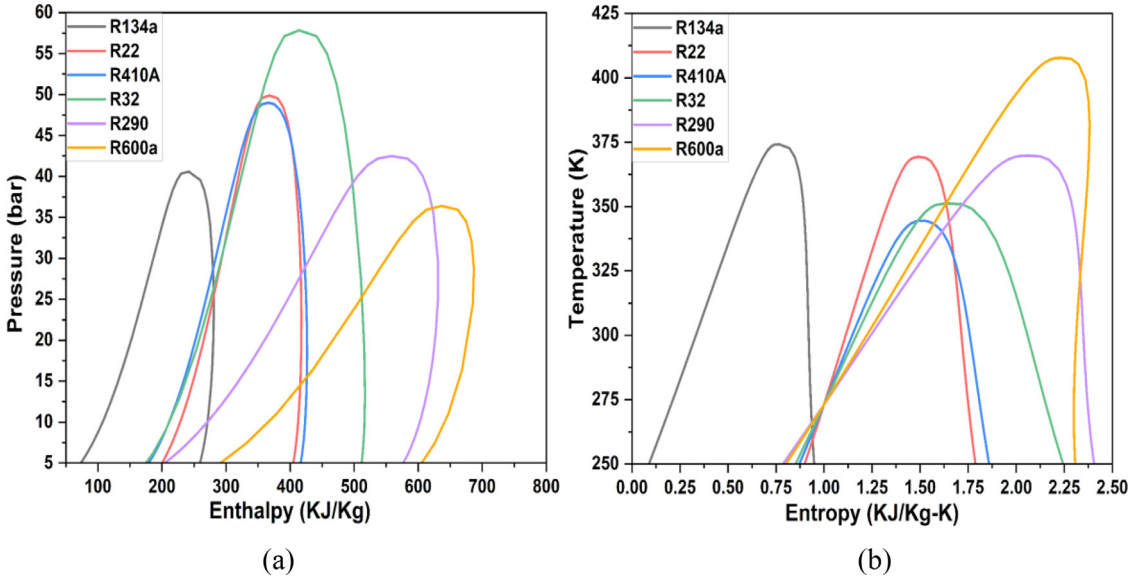

Fig. 1. Diagrams of (a) P-h and (b) T-s of the refrigerants investigated in this research activity.

est energetic (Joudi and Al-Amir, 2014). Another study compared the performance of R22, R290, R407A, and R410 in the residential air-conditioning unit and the results revealed that the power required for R290 is less than that of the other candidates, while R410 achieved the highest power required (Cheng et al., 2014). The COP of an air-conditioning system using R32 and R290 as a replacement for R22 and R410A was experimentally investigated, and the results exhibited that the COPs of R290 and R32 were higher than those of R22 and R410A (Zhou et al., 2010). In another study, R290 was investigated in an AC split unit and exhibited a higher energy efficiency ratio than that of R22 (Jierong and Tingxun, 2018).

Comparing R32 with the conventional refrigerants used in residential air conditioning systems is a key parameter to evaluate the relative performance and to assure that R32 meets the environmental and thermal criteria. From Table 1, This is clear R32, when compared with R134a and R410A, has a very high-pressure level and extremely high enthalpy, low-pressure drop in pipelines due to the low vapor density, low mass flow, and higher compressor discharge temperatures (Kibria et al., 2019). P-h diagram and T-s diagram comparison are shown in Fig. 1 for the investigated refrigerants.

3. Methodology

The research methodology for the proposed study involves both experimental and numerical activities to investigate the feasibility and reliability of using solar-powered air conditioners to cool a canopy at night-time. Experimental activities were performed utilising the conventional refrigerant "R134a" and its potential drop-in refrigerant "R290." At various condensation temperatures, testing procedures were carried out in order to assess the cycle's COP and exergetic efficiency. On the other hand, simulation modelling was employed in conjunction with a variety of modelling platforms in order to provide predictions regarding the overall performance of the system. TRNSYS was used to simulate the transient charging and discharging of batteries, and Integrated Environmental Solutions Virtual Environment (IESVE) was used to estimate the amount of solar energy that was required to power the unit. EES software was employed to predict the energetic and exergetic performance of the vapor-compression cycle using various working fluids. The simulated COP was validated using various statistical indices to verify the reliability of the simulation results.

4. System description

This study addressed various aspects, such as renewable energy, vapor compression cycle, and energy storage, in order to find a solution to the problem of meeting the demand for electricity required to power air conditioning systems in countries with extremely hot weather during summer months. The proposed system, depicted in Fig. 2, consists of three crucial units: a solar panel, an energy storage unit, and a VCC unit. The solar panels are roof-mounted and located outside. The external unit includes a compressor, a condenser, an expansion valve, and an energy storage system consisting of two 130 ah batteries connected in parallel with a charge controller and inverter. Due to technical barriers that can arise during the summer months in arid climates, which can shorten the battery life or cause damage, the battery is placed in the coolest external location and connected electrically to the system through wires. The batteries are also protected with a heat shield. The internal unit comprises an evaporator, external ducts, and an indoor canopy. Figure 3 depicts the P-h diagram of the VCC, which illustrates the operational processes of the system with R290 as the working fluid.

The stand-alone system contains internal and external components is illustrated in Fig. 4. The internal components comprise of the canopy,

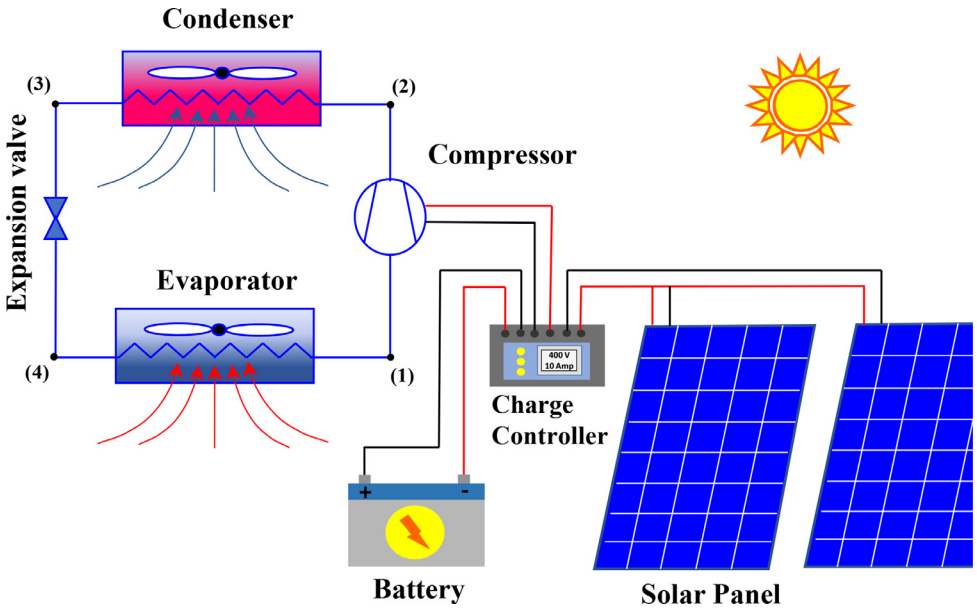

Fig. 2. The schematic of the proposed system comprises the power source, energy storage and the VCC.

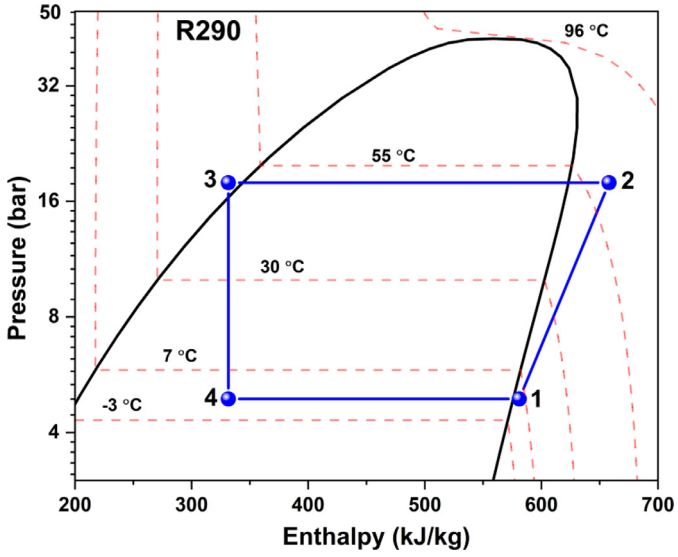

Fig. 3. P-h diagram for the proposed VCC cycle using R290.

supply and extract flex ducts and the AC unit. Aesthetics components were considered when designing the internal system to make it suitable for the end user and certain safety aspects such as rounded edges on the canopy.

5. Theoretical modelling

5.1. Solar calculation

One of the biggest challenges with utilising PV is the energy storage potential and thermal heat losses (Luerssen et al., 2020). Storing collected irradiance produced throughout the day can enable the energy to be distributed at times when there is no irradiance potential, night-time hours. A methodological approach to calculating the amount of solar energy on a given surface was investigated via Integrated Environmental Solutions Virtual Environment (IESVE). This commercial tool was chosen as it implements weather files and can easily calculate solar irradiance on surfaces. A simple model was constructed in IESVE to replicate the type of room in this study. The location file input was Abu Dhabi, a warm arid climate. The room dimensions are 3 m (W) by 4 m (D) by 2.5 m (H), this was modelled in ModelIT as a single zone. The east façade consisted of a 1m-by-1m single glazed 6mm window at an elevation 0.9m. The model was input to Apache in IESVE to look at the internal temperature within the room when no heating or cooling profile is applied. The results can be seen in Fig. 5. This simulation was run to indicate the internal room temperature profile throughout the year and show the zone overheating and thus the requirement for space cooling. There are 6,403 h out of the year, 73 percent, that the internal room temperature is greater than 25 °C.There are 5,648 h out of the year, 65 percent, where room temperature is greater than 28 °C. (CIBSE Guide A and TM52: The limits of thermal comfort), states that temperature should not exceed 28 °C for more than 1 percent of the occupied hours. This value is higher than a comfortable room temperature even at night-time and early mornings. The solar panel would be located on the roof of this building. The results for external surface incident solar power yield on the roof's surface are shown in Table 2.

5.2. Battery charging and discharging

The integration of solar photovoltaic (PV) and battery storage systems is an increasingly popular trend in the residential sector, mainly because it helps to achieve major goals such as reducing grid dependency and lowering emissions. In recent years deployment of PV and battery powered installations in the residential sector has increased (Khezri et al., 2022). The battery plays a crucial role in a solar – powered air conditioning system. It is charged by PV panels through a charge controller that regulates the current flow in and out of the energy storage. This device protects the battery from overvoltage, overcharging, and controls its discharge rate hence improving its life, performance and safety (Vignesh et al., 2019). Today's market offers various kinds of electricity storage technologies with different chemistries. However, lead batteries are well – established technology for industrial applications and can be used successfully as utility energy storage. One of the biggest advantages of lead batteries is their long cycle and lifespan. Additionally, lead is the most widely recycled metal, and lead batteries are almost fully recyclable, with nearly 99% of those batteries being collected and recycled in the USA and Europe (May et al., 2018). Taking into consideration those benefits, it was decided to use lead – acid batteries as energy storage for this project. The electricity generated by two PV panels throughout the day is stored in this battery and used at night to power AC unit, which runs continuously for about five hours off – grid and consumes around 3 kWh during that time.

Table 2
The total annual solar power yield potential for the example building.

Date	Direct radiation (kWh/m^2)	Roof area (m^2)	Direct radiation on roof (W/m^2)	Surface incident, solar energy, roof (MWh)	PV efficiency (%)	Total Solar power yielded (kWh)
Jan 01-31	26.75	12	321	0.2284	0.15	34.26
Feb 01-28	13.52	12	162.24	0.2965	0.15	44.475
Mar 01-31	84.36	12	1012.32	0.833	0.15	124.95
Apr 01-30	85.65	12	1027.8	1.149	0.15	172.35
May 01-31	118.78	12	1425.36	1.598	0.15	239.7
Jun 01-30	107.74	12	1292.88	1.6351	0.15	245.265
Jul 01-31	61.73	12	740.76	1.3186	0.15	197.79
Aug 01-31	96.67	12	1160.04	1.3339	0.15	200.085
Sep 01-30	74.23	12	890.76	0.9079	0.15	136.185
Oct 01-31	68.64	12	823.68	0.6316	0.15	94.74
Nov 01-30	23.87	12	286.44	0.2353	0.15	35.295
Dec 01-31	21.88	12	262.56	0.1621	0.15	24.315
Total	783.81	12	9405.72	10.3294	0.15	1549.41

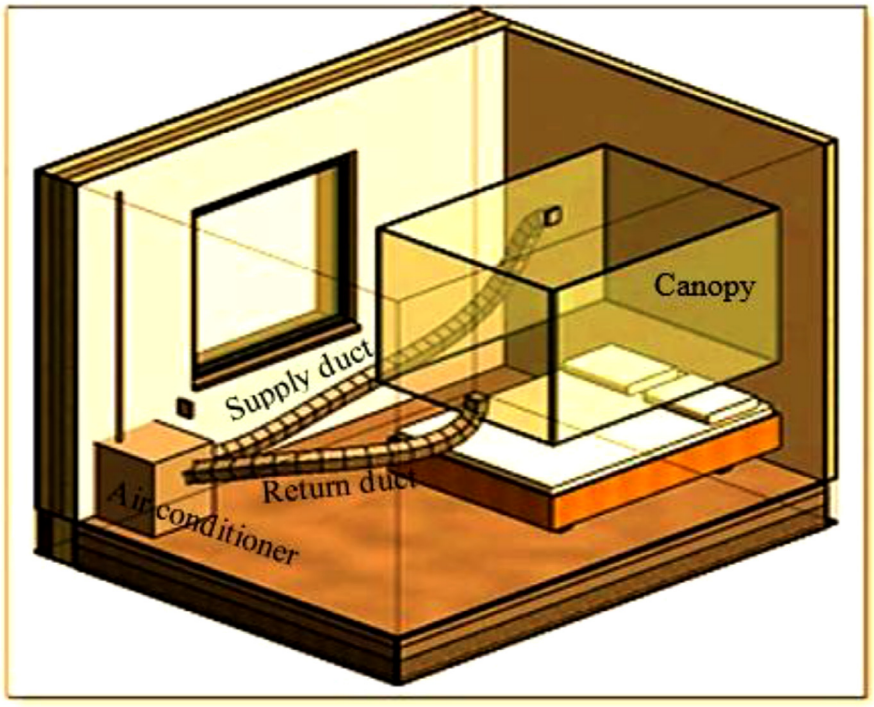

Fig. 4. Room layout showing system layout, and 3D view of a typical bedroom.

The annual solar power yield of the 3.5 m^2 panels simulated in IESVE, was sufficient for the electrical storage used in the simulation comprised of a 2 No. 130 Ah and 12 V lead acid batteries which were charged by a two 400 W monocrystalline PV panels, the electricity consumption of the AC unit was around 500 W.

Figure 6 illustrates a weekly profile of an air conditioning unit's battery charging and discharging versus variations in total horizontal radiation (red line) and ambient temperature (black line). The meteorological data file was configured to reflect August weather conditions in Abu Dhabi. The results showed that the unit's battery was charged to a sufficient level in approximately 8.5 hrs each day, as represented by the blue line in the graph, to allow for seven hours of continued operation during the night. The simulation demonstrated that the batteries charged by the solar panels are capable of supporting the air conditioning unit during the night.

5.3. Vapor compression cycle calculation

In the research's theoretical section, three different software programs were utilised to demonstrate the system's principle: IES, TRNSYS, and EES. The software EES was essential to simulate the VCC and evaluate the energetic and exergetic efficiency of the system.

The thermodynamic efficiency of the working fluid is the primary basis for creating a model of an air conditioning system. In order to select the suitable refrigerant for the system, a comparison simulation of different refrigerants was performed to identify the suitable thermodynamics characteristics for the A-C unit. The model was developed on EES to design the system and carry out a simulation between different refrigerants. The minimum superheat is required to get a dry compression and that is depends on the refrigerant type, isentropic efficiency, and the condensation and evaporation temperature of the unit. The results show the energetic and exergetic performance of the VCC using different refrigerants (see Table 4) that were subjected to the same assumptions and input parameters as follows:

- The unit at steady state condition
- The pressure drops in the cycle component are neglected.
- The heat loss in the piping, compressor, and expansion valve are neglected.
- The isentropic efficiency of the hermetic compressor is assumed to be 0.8.

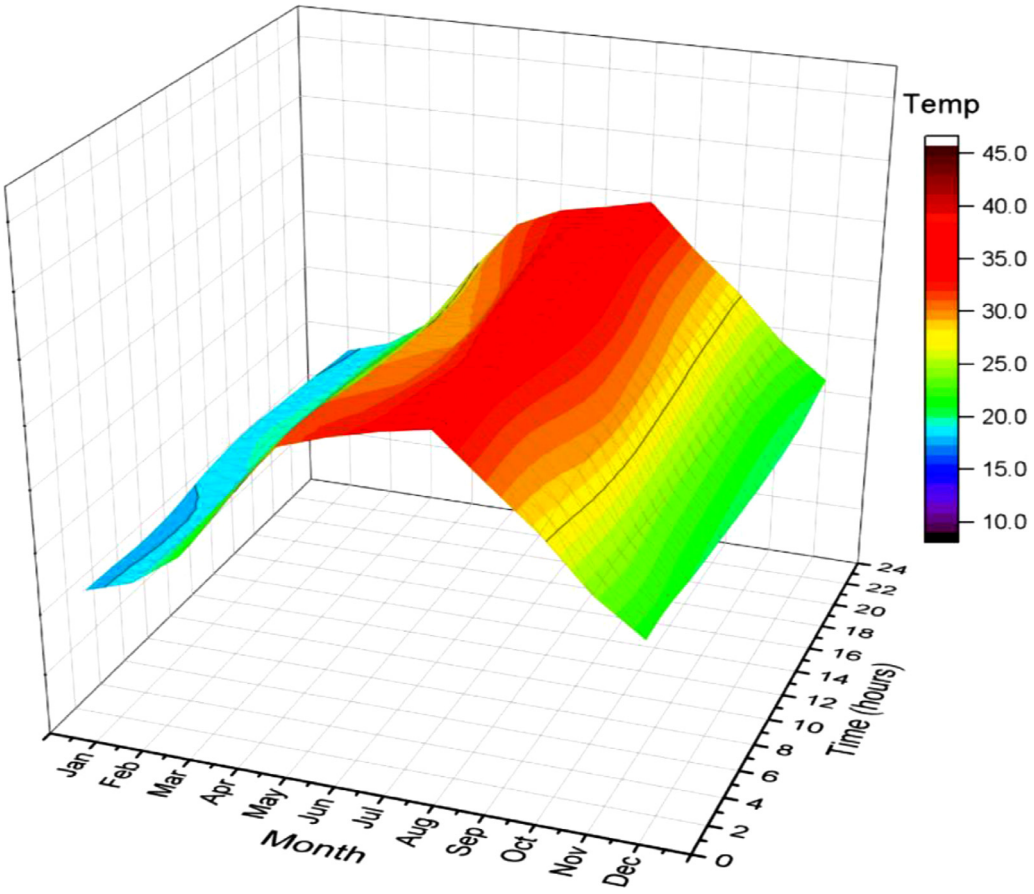

Fig. 5. The annual internal air temperature for the IESVE apache simulation model.

- Expansion process is isenthalpic expansion $h_3 = h_4$

The heat load on the AC unit (q_{tot}) can be divided into three sources: the heat conducted through the canopy material (q_{cd}), the heat contained in the supplied fresh air (q_a) and the heat released by occupants (q_{occ}), which can be determined as follows:

$$q_{cd} = U A(\Delta T) \tag{1}$$

$$U = \frac{1}{\frac{1}{\alpha_{in}} + \frac{t}{k} + \frac{1}{\alpha_{out}}} \tag{2}$$

$$q_a = \dot{m}_a(\Delta h) \tag{3}$$

$$q_{tot} = q_{cd} + q_{sa} + q_{occ} \tag{4}$$

The material recommended for the canopy is aluminium foil/bubble composites of 0.0392 W/(m-K) thermal conductivity (Uvsløkk et al., 2017). The heat produced by occupants sedentary is 100W per person and the recommended air supply to canopy is 8 l/s per person (ASHRAE, 2004).

In addition, the specific work required to circulate the refrigerant (ẇ) can be obtained from the difference in enthalpy at the inlet and outlet of the compressor, whilst the refrigerant effect (RE), on the other hand, can be determined from the difference in enthalpy at the inlet at outlet of the evaporator as shown in Eqs. (5) and (6), respectively.

$$w = h_{comp,out} - h_{comp,in} \tag{5}$$

$$RE = h_{evap,out} - h_{evap,in} \tag{6}$$

By knowing the total heat load and the refrigeration effect, the refrigerant flow rate required can be therefore determined from:

$$\dot{m}_r = \frac{q_{tot}}{RE} \tag{7}$$

By assuming the isentropic efficiency (~ 0.8), the actual power drawn by the compressor can be calculated as follows:

$$P_{comp} = \frac{\dot{m}_r(h_{2,ise} - h_1)}{\eta_{ise}} \tag{8}$$

The theoretical COP can be calculated based on the modelling results:

$$COP_{th} = \frac{h_1 - h_4}{h_2 - h_1} \tag{9}$$

The average temperature in condenser and evaporator can be obtained by Eqs. (10) & (11) in order to calculate the exergy efficiency by the system,

$$T_{Cond,\ ave} = \frac{h_2 - h_3}{s_2 - s_3} \tag{10}$$

$$T_{evap,\ ave} = \frac{h_1 - h_4}{s_1 - s_4} \tag{11}$$

The rate of exergy output is calculated using Eq. (12), and the total exergy destruction is calculated using Eq. (13)

$$E_{out} = \left[1 - \frac{T_0}{T_{Cond,ave}}\right] \cdot \dot{Q}_{Cond} - \left[1 - \frac{T_0}{T_{evap,evap}}\right] \tag{12}$$

$$Ex_{dest,total} = T_0 \left[\frac{\dot{Q}_{Cond}}{T_{Cond,ave}} - \frac{RE}{T_{evap,evap}}\right] \tag{13}$$

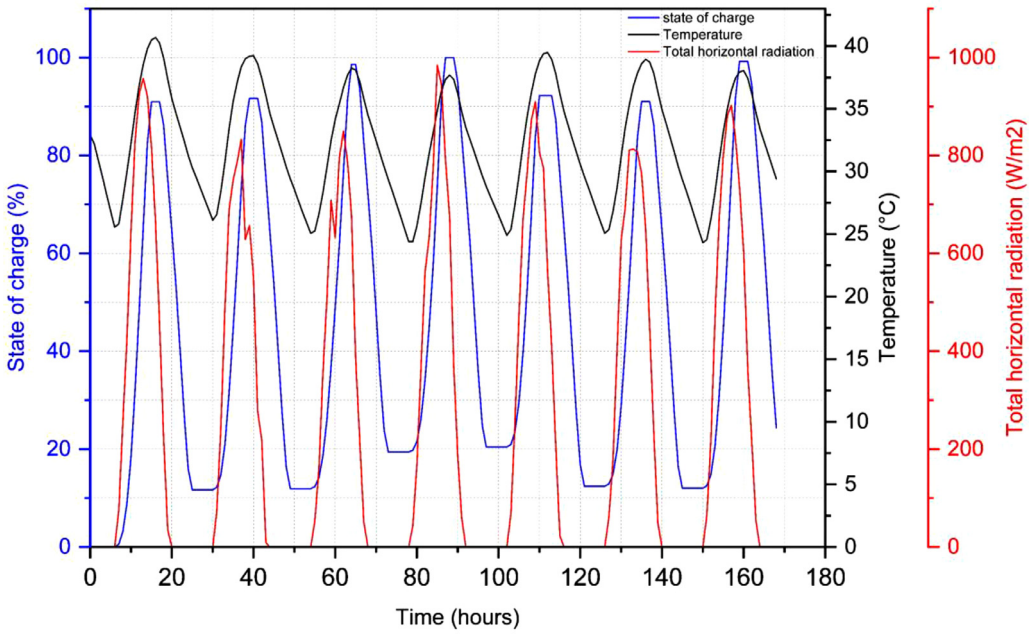

Fig. 6. Battery state of charge Vs diffused radiation and ambient temperature.

Table 3
Component dimensions and size provided by Eberspaecher.

Component	Type	Dimensions	Weight	Power Supply
Compressor	A 1/3 horsepower brushless DC Variable Speed Compressor. Discharge, displacement 7.1 cm^3 Compression Ratio 8:1.	(154 × 130 × 152)*mm*. 3/8" ID Suction - 5/16" ID Discharge, and HBP A/C, Maximum.	4.8 kg	24/48V DC.
Condenser	A forced air condenser with a type of: COND 2501 MF 24V	(458 × 367 × 132) *mm*	7 kg	24 V & 4.5 Amps
Evaporator	evaporator EV 4000 G1.5 – cooling only	(390 × 235 × 135) *mm* TXV connection on right side (air flow direction): Suction no. 12; liquid no. 6. Drain water socket: 2 x ø 10.35 mm	3.8 kg	24 V & 4.5 Amps. Air flow of 450 m^3/hr
Battery	LAGM-130-12V 130 Ah	W x H x D (330 × 175 × 210) mm	28 kg	12 V x 2 / 24 V
Solar Panel	2 x SPR-MAX3- 400 Mono Solar panel	W x Hx D 1690 × 1046 × 40 (mm)	2 × 19 kg	2 × 400W

The exergy efficiency of the vapor Compression cycle

$$\eta_{ex} = \frac{E_{out}}{W_{actl}} \tag{14}$$

System daily Power consumption is calculated according to Eq. (15)

$$D_C = R_t \times W_{act} \tag{15}$$

The Battery charging voltage (If I >0) is obtained using Eq. (16)

$$V = e_{qc} - g_c(1-F) + Ir_{qc}\left(1 + \frac{m_c(1-F)}{\frac{Q_c}{Q_m} - (1-F)}\right) \tag{16}$$

The Battery discharging mode (If I <0) is obtained using Eq. (17)

$$V = e_{qd} - g_d(1-F) + Ir_{qd}\left(1 + \frac{m_d(1-F)}{\frac{Q_d}{Q_m} - (1-F)}\right) \tag{17}$$

6. Experimental setup and procedure

Figure 7 illustrates the laboratory scale of the vapor compression cycle of an air-conditioning bed unit. The VCC components were used are commercially available and provided by Eberspaecher company without any modifications. According to the technical specification provided by the design calculation agreed before, the following components (Table 3) are selected carefully in order to carry out the final scale of the experiment and thus the results. The compressor, condenser and evaporator fan motor are using a 24V power supply. The reason for choosing 24V is that the 24V power supply is more compatible with AC appliances and greatly reduces the wiring cost to almost half the original cost. Using a 24V power supply decreases the number of batteries that would be used compared to a 48V power supply, this is because most of the batteries are 12V. At 24V 2 batteries would be required in series whereas for a 48V power supply would require 4 batteries to be connected in series.

The product will be running during the summertime. Operating temperature range for the product will be between 35°C to 40°C. The operating humidity range for this product during the summertime between 50% to 60%.

The experimental setup consists of a VCC, a tent to replace a room, two heaters, double-bed, and a canopy above the bed. The components are integrated as one unit in an HVAC workshop and charged with the available refrigerant R134a which is used as a reference refrigerant. Heating up the tent up to 40°C using an electric heater was necessary to get a similar environmental temperature of the middle eastern countries. The AC/DC converter and battery supplied the unit by the adequate energy to keep the unit running smoothly. The flexible ducts worked as an intermediate connecter between the forced-air evaporator and the canopy above the bed in order to supply a cold air to the canopy. 2 × 100 W green- house heaters were placed inside the canopy to replace two persons sleeping on bed. A digital thermostat and timer

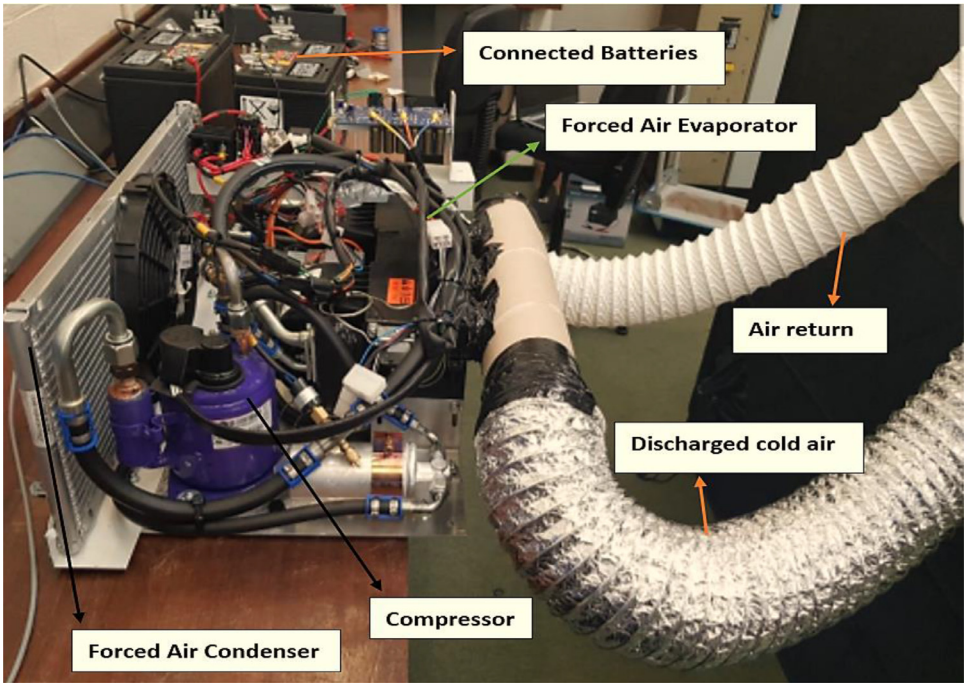

Fig. 7. The scale of VCC unit during the experimental activities.

were placed to measure the temperature inside the canopy while the unit is running which is necessary to obtain the temperature reduction rate inside the bed canopy. After heating up the canopy and the tent to $45°C$ which is the maximum environmental temperature the unit will run in middle eastern countries during the night-time, the AC unit was operated in steady state conditions. The batteries were charged to the maximum limit using the charging machine. A shunt meter was placed between the batteries and the unit to measure the current to the load. The unit is running, and the results are recorded.

7. Validation

The validity of the simulation results for the A-C bed unit model was assessed by comparing experimental COP outcomes to statistical indices within an acceptable level of tolerance. In addition, experimental results for R290 and R134a at condensation temperatures ranging from 37 to 55 ˚C were validated. To ensure that the testing sets were identically matched, the model was executed at the same experimental condensation temperature as the experiment. In addition, three statistical indicators were used to verify and evaluate the reliability of simulation results: Percent Error (% Error), coefficient of determination (R^2), and root mean square error (RMSE). The following equations define the mathematical characteristics of the three statistical indices.

$$\%\ \text{Error} = \left(\frac{Y_{Num} - Y_{Exp}}{Y_{Exp}}\right) \times 100 \tag{18}$$

$$R^2 = \frac{\sum_{j=1}^{n}\left(Y_{Num} - \bar{Y}_{Exp}\right)}{\sum_{j=1}^{n}\left(Y_{Exp} - \bar{Y}_{Exp}\right)} \tag{19}$$

$$RMSE = \sqrt{\frac{\sum_{i=0}^{n}\left(Y_{Exp} - Y_{Num}\right)^2}{n}} \tag{20}$$

where, Y_{Num} are the numerical values, Y_{Exp} the experimental values, $\bar{Y}_{Exp}$ the average experimental values and n is the number of reference data.

Figure 8(a) and (b) illustrate the statistical results as the coefficients of determination R^2 of COP for R290 and R134a at various condensation temperatures, which are 0.999 and 0.999, respectively. Furthermore, the statistical analysis reveals a close relationship between the experimental points and the regression line, indicating that the simulated COP values are consistent with the experimental values and that the simulation model can be relied upon for future predictions.

The statistical analysis results depicted in Fig. 7(a) and (b) for the two testing sets confirmed that the error percentage of the simulated model employing R290 and R134a is less than 5%. In addition to the statistical outcomes of R^2 and percentage error, the RMSE values for R290 and R134a between empirical and simulated data for the two testing sets are consistent, with values of 0.0042 and 0.0022, respectively. Consequently, the simulation results validate the model's high COP prediction accuracy.

8. Results and discussion

8.1. Theoretical results

Table 4. depicts the theoretical results of the VCC simulated in EES at various condensation temperatures and fixed evaporation temperatures. Alongside the cycle's energetic performance, the exergetic performance outlines the feasibility and possibility of conducting experimental activity development.

The cycle's COP is influenced by the values of the compressor discharge temperature, the system mass flow rate, and the compressor isentropic efficiency. The discharge temperature of the compressor is proportional to the isentropic exponent of the refrigerant. The higher the isentropic exponent of the refrigerant, the higher the discharge temperature and thus the higher the compressor input power. R32 presented the highest isentropic exponent value of 1.252 and thus very high discharge temperature. R600a, on the other hand, demonstrated the lowest compressor discharge temperature due to its lowest isentropic exponent value and dry refrigerant type (Sulaiman et al., 2022), which requires a specific minimum degree of superheat before the compression process to ensure dry compression (Fig. 9(a)).

The system mass flow rate, which is a function of the heat load and cycle REs, presented the highest value when R134a and R410A are employed as working fluids. The higher the system temperature lift the higher the mass flow rate and thus the compressor input power, see Fig. 10(a). Theoretical findings indicated that R32 and R410A required

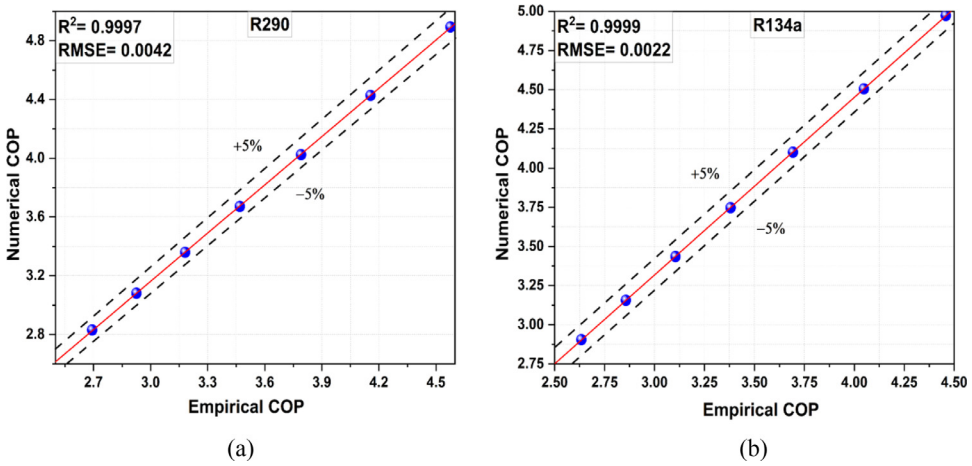

Fig. 8. Validation of the numerical COP VS empirical COP values for (a) R290 and (b) R134a, at condensation temperatures ranging from 37 to 55 °C with a 3 K temperature increment.

Table 4
The results of VCC Air conditioning bed unit using EES.

= 36 K, T_{cond} = 37 °C							ΔT_{lift} = 54 K, T_{cond} = 55 °C					
Refrigerant	T_{dis} (°C)	P_r [-]	W_{in} (hP)	RE (KJ/kg)	COP [-]	η_{ex} %	T_{dis} (°C)	P_r [-]	W_{in} (hP)	RE (KJ/kg)	COP [-]	η_{ex} %
R134a	49.5	3.09	0.184	155.8	4.97	57.72	70.4	4.91	0.314	128.7	2.91	47.8
R22	63.7	2.77	0.185	167	4.95	57.42	90.8	4.23	0.311	142.8	2.94	48.3
R410A	61.1	2.73	0.195	171.5	4.68	54.34	87.7	4.17	0.351	137.1	2.6	42.77
R32	76.1	2.74	0.192	257.9	4.76	55.3	109.8	4.19	0.331	219.4	2.76	45.42
R290	49	2.61	0.187	293.4	4.89	56.8	69.59	3.9	0.32	240.5	2.83	46.6
R600a	44	3.02	0.18	285.3	5.08	58.92	60.85	4.76	0.303	239	3.01	49.49

the highest input power to the compressor due to higher values of the isentropic exponent and pressure ratio, as shown in Fig. 10(b). In comparison to the other participants, the cycle employed R600a presented the lowest input power. The theoretical results confirmed that the input power for all participants was less than 1/4 hP at a condensation and lift temperatures of 48 °C and 45 K, respectively. Whereas, at values of 56 °C and 53 K, respectively, the compressor's input power yielded less than 1/3 hP for all participants except the cycle utilised R410A as working fluid. The results indicated that increasing the system temperature lift increased the system pressure ratio and consequently the drawn power of the compressor increased .

RE is an essential consideration of residential mini-split air conditioning systems, and it is related to the value of refrigerant's latent heat of vaporisation. R290 represents the highest latent heat of vaporisation and thus a higher refrigerant effect, followed by R600a. R134a, on the other hand, demonstrated the least RE due to its low latent heat of vaporisation (Fig. 9(b)). The results also revealed that the higher the refrigerant effect, the higher the system's COP, and conversely. According to the findings, increasing the temperature lift of the system decrease the RE of the system . The system RE value, as well as the theoretical power input, are the two most important factors in determining system COP. Theoretical findings indicated that increasing the condensation temperature reduces the system COP. This is due to the fact that increasing the condensation temperature at constant evaporation temperature increases the system temperature lift, thereby increasing the compressor's theoretical input power.

At different condensation temperatures, R600a presented the highest COP value, while R410A showed the lowest COP value, according to the theoretical results (Fig. 11(b)). This is due to the fact that R600a combines the system advantages of low input power and high value of RE. Correspondingly, the system employing R600a demonstrated the highest exergetic efficiency among the other refrigerant candidates. On other

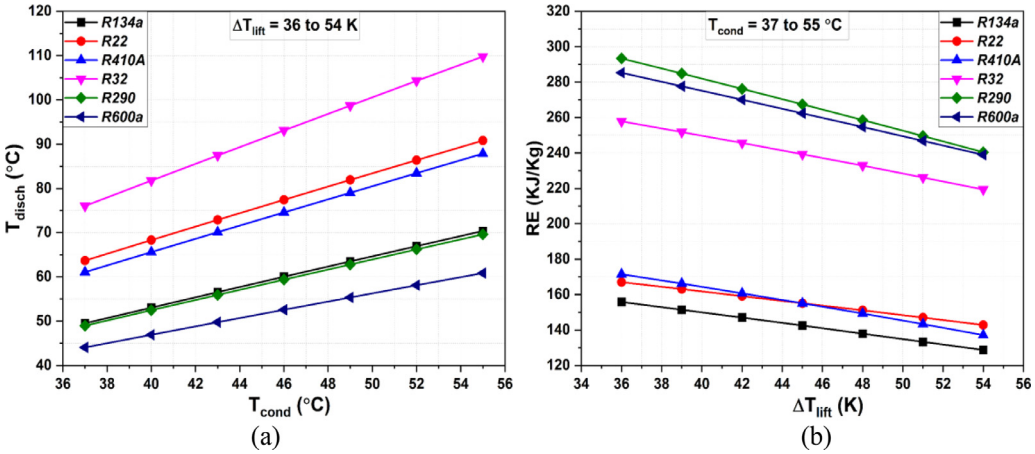

Fig. 9. (a) the discharge temperature Vs Condensation temperature and (b) the refrigerant effect Vs temperature lift.

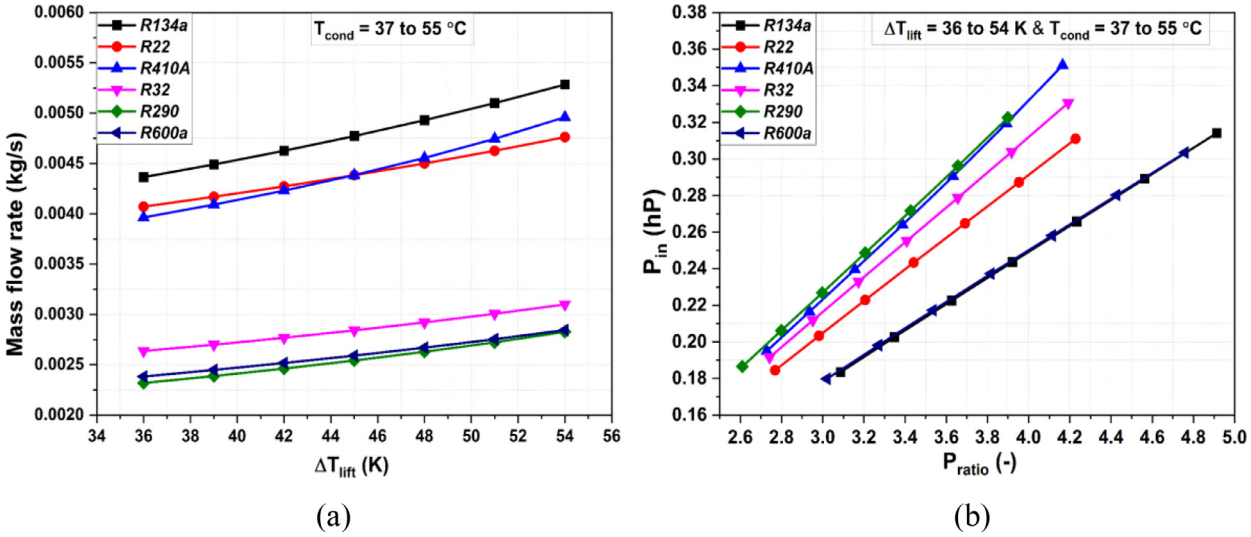

Fig. 10. (a) the system mass flow rate Vs temperature lift and (b) the pressure ratio Vs input power of the compressor.

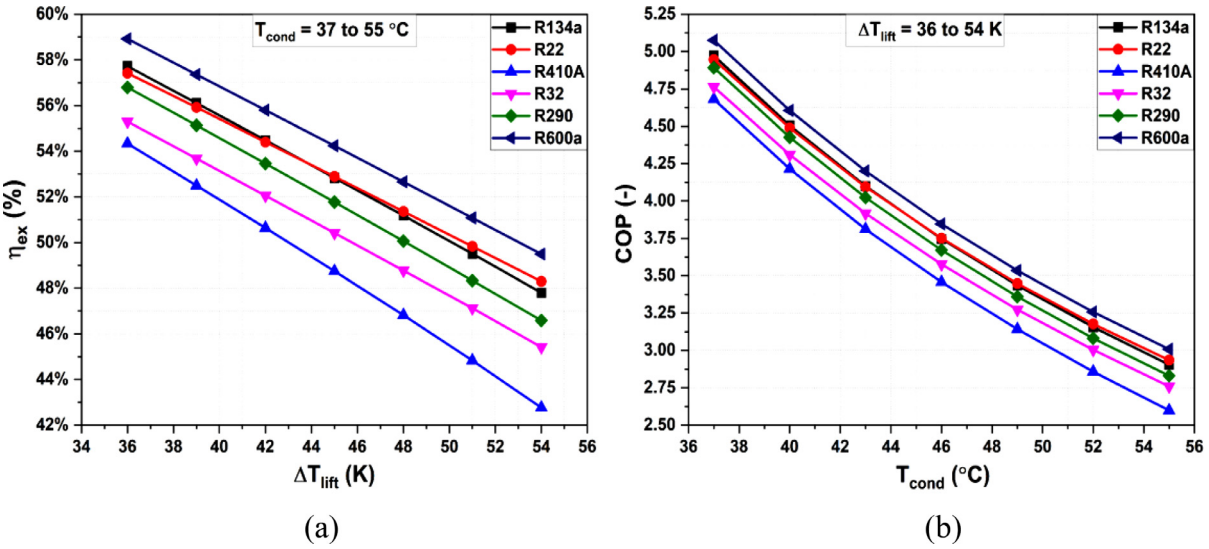

Fig. 11. (a) exergy efficiency Vs temperature lift and (b) the COP Vs condensation temperature.

hand, the system employing R410A and R32 as refrigerants showed the least exergetic destruction and exergetic efficiency. The results indicate that the higher the system temperature lift the lower exergetic efficiency of the system (Fig. 11(a)).

8.2. Experimental results

The primary objective of this experimental setup was to demonstrate the potential and dependability of running an off-grid A/C unit and providing a comfortable environment to bed-canopy occupants for at least six hours. In addition, an eco-friendly refrigerant was tested and evaluated to effectively supersede the convectional working fluids used in A/C units. R290 was used as a comparison refrigerant to R134a under similar environmental and technical input parameters. The testing unit was developed to operate at temperatures ranging from 33 to 45 °C in order to simulate the extremely hot climate environmental conditions reported in the Middle Eastern countries during the summer season. Table 5 shows the practical performance of the VCC with the results of R134a and R290 as eco-friendly suitable alternative refrigerants. Seven runs were performed using R134a and R290 at a condensation temperature of 52 °C and a temperature lift of 51K. The COP standard deviation for R134a runs was ±0.0395, whereas the COP standard deviation for R290 runs was ±0.0481.

Due to the reduction in practical isentropic efficiency of the compressor compared to the calculated theoretical efficiency, the testing findings for both refrigerants exhibited higher discharge temperatures than those obtained from the theoretical results. As a result, the compressor's practical input power rised, reducing the system's practical COP. According to the test results for both refrigerants, heat exchanger pressure drops caused a minor decrease in the system's suction pressure, resulting in an increase in the system's practical pressure ratio. The measured RE of the unit, on the other hand, is greater than the values obtained from the theoretical results. This is due to the fact that as the system's practical pressure decreased through the heat exchangers, the evaporation latent heat line on the P-h diagram shifts downward away from the critical temperature, resulting in a higher latent heat value represented by the longer line on P-h diagram. Despite the fact that the practical RE is slightly higher for both refrigerants, the COP is lower than the theoretical COP due to the unit's considerable increase in practical input power. According to the testing results, decreases in practical COP resulted in a noticeable decrease in overall system exergetic efficiency of 4% to 6%. The findings demonstrate the significance of temperature lifts in

Table 5
The experimental results of the A/C test rig using two working fluids.

R134a : ΔT_{lift} = 36 to 51 K						R290: ΔT_{lift} = 36 to 51 K					
T_{cond} (°C)	T_{dis} (°C)	P_r [-]	W_{in} (hP)	COP [-]	η_{ex} %	T_{cond} (°C)	T_{dis} (°C)	P_r [-]	W_{in} (hP)	COP [-]	η_{ex} %
37	53.21	3.234	0.2048	4.458	54.46	37	51.5	2.77	0.1995	4.576	55.91
40	56.84	3.507	0.2255	4.048	53.07	40	54.98	2.971	0.2196	4.156	54.48
43	60.44	3.798	0.2471	3.693	51.65	43	58.43	3.182	0.2408	3.791	53.01
46	64.01	4.107	0.2699	3.381	50.19	46	61.85	3.403	0.2631	3.469	51.48
49	67.55	4.434	0.294	3.105	48.7	49	65.26	3.636	0.2868	3.182	49.91
52	71.07	4.78	0.3194	2.857	47.18	52	68.64	3.881	0.312	2.926	48.3

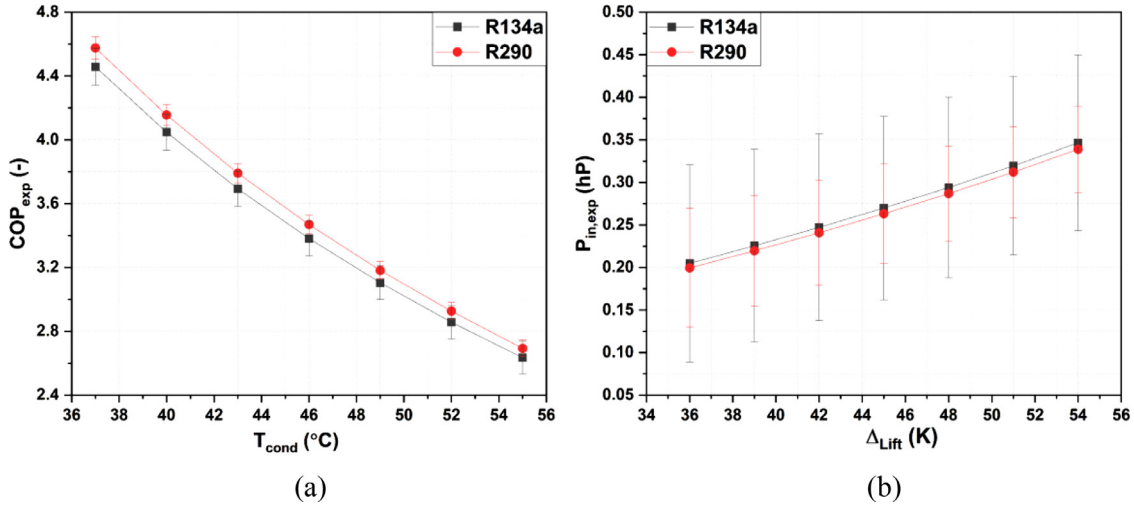

Fig. 12. the percentage error of (a) COP and (b) the input power, as a function of condensation temperature and temperature lift respectively.

determining the COP, the lower the temperature lift, the higher the cycle COP. According to the experimental outcomes, the unit draws less than 1/3 hP at various condensation temperatures using R290. The findings of the test results confirmed the theoretical results of the technical and environmental advantages of using R290 as a replacement for the banned refrigerants. The estimated percentage error values of the COP at different condensation temperatures were found to be at a tolerance of ±11.6% for R134a. In comparison, the percentage error values for the COP using R290 was around ±7% (Fig. 12).

9. Conclusion

This paper provides a comprehensive numerical and empirical analysis to assess the practicability of operating an off-grid air-conditioning bed unit with low GWP refrigerants. The simulation analysis and experimental activities has been carried out using a mechanically driven single-stage VCC and at different condensation temperatures. To identify the most efficient and optimal refrigerants, the analysis considered the energetic and exergetic performance of the mechanically driven air conditioning unit under various cycle operational conditions. The primary conclusions based on the experimental and numerical findings are as follows:

- The thermodynamic and transport properties of the ecologically friendly refrigerants R600a and R290 are comparable to those of investigated candidates. In addition to their low GWP values, R600a and R290 are confirmed as suitable replacement refrigerants for R134a and R410A based on the higher values of COP and RE at different operational temperatures.
- The VCC air-conditioning bed-unit system employing R600a as a refrigerant would require specific mapping for the minimum superheat degree to the compressor, thereby necessitating the addition of an internal heat exchanger to ensure a dry compression process.
- The COP indicates the maximum value for all candidates as the temperature lift decreases. Reducing the temperature lift between evaporator and condenser enhances the performance of the system.
- Increasing the temperature lift will cause the condensation line to shift closer to the critical point (dome), resulting in a shorter condenser line and a shorter evaporation line on the P-h diagram and, consequently, a lower RE value.
- Compared to R134a, the experimental COP of R290 improved by 2.42 %, with less input work of 2.31 % and greater exergetic efficiency of 2.37 %.
- When the condensation temperature increased from 37 to 52 °C, the experimental exergetic efficiency and the system COP declined by 13.6% and 36.1%, respectively.
- After conducting both numerical and experimental tests using R290, it was found that the system required less than one-third horsepower to operate, and the 2 × 130 Ah batteries had enough charge to run the system for 7 h after been fully charged. These results indicate that the unit is practically feasible.

Declaration of Competing Interest

The authors declare that they have no known competing financial interests or personal relationships that could have appeared to influence the work reported in this paper.

Data availability

Data will be made available on request.

Acknowledgments

The authors gratefully acknowledge the support from Techstart Ventures NI, as well as the support from Department for the Economy

(Northern Ireland, EP/T022981/1) DEcarbonisation of Low TemperATure Process Heat Industry, DELTA PHI and EP/R045496/1 Low Temperature Heat Recovery and Distribution Network Technologies (LoTNET).

References

Agreement, P., 2015. UNFCCC, Adoption of the Paris agreement. COP. 25th Session Paris.

Al-Alili, A., Hwang, Y., Radermacher, R., Kubo, I., 2012. A high efficiency solar air conditioner using concentrating photovoltaic/thermal collectors. Appl. Energy 93, 138–147.

Al-Yasiri, Q., Szabó, M., Arıcı, M., 2022. A review on solar-powered cooling and air-conditioning systems for building applications. Energy Rep. 8, 2888–2907.

Allamraju, K., 2013. Materials used for renewable energy resources. Adv. Mater. Manuf. Charact. 3, 243–248.

Allen, M. Antwi-Agyei, P., Aragon-Durand, F., Babiker, M., Bertoldi, P., Bind, M., Brown, S., Buckeridge, M., Camilloni, I., Cartwright, A., 2019. Global warming of 1.5 °C. An IPCC Special Report on the impacts of global warming of 1.5 °C above pre-industrial levels and related global greenhouse gas emission pathways, in the context of strengthening the global response to the threat of climate change, sustainable development, and efforts to eradicate poverty.

ASHRAE, 2020. Update on New Refrigerants Designations and Safety Classifications, ANSI/ASHRAE Standard 34-2019.

ASHRAE, A.H., 2004. HVAC systems and equipment. Refrig. Air Cond. Eng., SI ed.. American Society of Heating, Atlanta, GA.

Brückner, S., Liu, S., Miró, L., Radspieler, M., Cabeza, L.F., Lävemann, E., 2015. Industrial waste heat recovery technologies: an economic analysis of heat transformation technologies. Appl. Energy 151, 157–167.

Chen, J.M., 2021. Carbon neutrality: toward a sustainable future. Innovation 2, 100127.

Cheng, S., Wang, S., Liu, Z., 2014. Cycle performance of alternative refrigerants for domestic air-conditioning system based on a small finned tube heat exchanger. Appl. Therm. Eng. 64, 83–92.

Chua, K.J., Chou, S.K., Yang, W.M., Yan, J., 2013. Achieving better energy-efficient air conditioning - a review of technologies and strategies. Appl. Energy 104, 87–104.

Clerici, A., Alimonti, G., 2015. World energy resources. In: EPJ WEB of Conferences. EDP Sciences, p. 1001.

EIA, 2021. Pathway to Net-Zero Cooling Product List.

El-Morsi, M., 2015. Energy and exergy analysis of LPG (liquefied petroleum gas) as a drop in replacement for R134a in domestic refrigerators. Energy 86, 344–353.

Eveloy Valerie and Yusra Alkendi, 2021. Solar compression-assisted multi-ejector indoor air conditioning system for hot climate conditions.

Fawzy, S., Osman, A.I., Doran, J., Rooney, D.W., 2020. Strategies for mitigation of climate change: a review. Environ. Chem. Lett. 18, 2069–2094.

Fong, K.F., Lee, C.K., Chow, T.T., 2011. Improvement of solar-electric compression refrigeration system through ejector-assisted vapour compression chiller for space conditioning in subtropical climate. Energy Build. 43, 3383–3390.

Ghodbane, M., Boumeddane, B., Hussein, A.K., 2021. Performance analysis of a solar–driven ejector air conditioning system under EL-Oued climatic conditions. Algeria. J. Therm. Eng. 7, 172–189.

Ianc, N., Boantă, C., Gherghe, I., Tomescu, C., 2020. Environmental impact of methane released from coal mines. MATEC Web Conf. 305, 00030.

IEA, 2018. The future of cooling opportunities for energy- efficient air conditioning.

Isaifan, R.J., Baldauf, R.W., 2020. Estimating economic and environmental benefits of urban trees in desert regions. Front. Ecol. Evol. 8, 16.

Jierong, L., Tingxun, L., 2018. Detailed dynamic refrigerant migration characteristics in room air-conditioner with R290. Int. J. Refrig. 88, 108–116.

Johnson, E., 1998. Global warming from HFC. Environ. Impact Assess. Rev. 18, 485–492.

Joudi, K.A., Al-Amir, Q.R., 2014. Experimental Assessment of residential split type air-conditioning systems using alternative refrigerants to R-22 at high ambient temperatures. Energy Convers. Manag. 86, 496–506.

JRAIA, 2022. Estimates of world air conditioner demand the japan refrigeration and air conditioning industry association.

Khezri, R., Mahmoudi, A., Aki, H., 2022. Optimal planning of solar photovoltaic and battery storage systems for grid-connected residential sector: review, challenges and new perspectives. Renew. Sustain. Energy Rev. 153, 111763.

Kibria, M.T., Islam, M.A., Saha, B.B., Nakagawa, T., Mizuno, S., 2019. Assessment of environmental impact for air-conditioning systems in japan using HFC based refrigerants. Evergreen 6, 246–253.

Lemmon, E.W., McLinden, M.O., … Huber, M.L., 2010. NIST Reference Fluid Thermodynamic and Transport Properties—REFPROP .v9.0. NIST, Gaithersburg, MD.

Luerssen, C., Gandhi, O., Reindl, T., Sekhar, C., Cheong, D., 2020. Life cycle cost analysis (LCCA) of PV-powered cooling systems with thermal energy and battery storage for off-grid applications. Appl. Energy 273, 115145.

May, G.J., Davidson, A., Monahov, B., 2018. Lead batteries for utility energy storage: a review. J. Energy Storage 15, 145–157.

Mota-Babiloni, A., Navarro-Esbrí, J., Makhnatch, P., Molés, F., 2017. Refrigerant R32 as lower GWP working fluid in residential air conditioning systems in Europe and the USA. Renew. Sustain. Energy Rev. 80, 1031–1042.

Nasa, 2022. Heatwaves and Fires Scorch Europe, Africa, and Asia [WWW Document]. URL https://earthobservatory.nasa.gov/images/150083/heatwaves-and-fires-scorch-europe-africa-and-asia (accessed 4.1.23).

O'Neill, B.C., Kriegler, E., Ebi, K.L., Kemp-Benedict, E., Riahi, K., Rothman, D.S., van Ruijven, B.J., van Vuuren, D.P., Birkmann, J., Kok, K., 2017. The roads ahead: narratives for shared socioeconomic pathways describing world futures in the 21st century. Glob. Environ. Chang. 42, 169–180.

Pham, H.M., Rajendran, R., 2012. R32 and HFOs as low-GWP refrigerants for air conditioning.

Santamouris, M., 2015. Regulating the damaged thermostat of the cities - Status, impacts and mitigation challenges. Energy Build. 91, 43–56.

Santamouris, M., Feng, J., 2018. Recent progress in daytime radiative cooling: Is it the air conditioner of the future? Buildings 8.

Sulaiman, A.Y., Cotter, D.F., Le, K.X., Huang, M.J., Hewitt, N.J., 2022. Thermodynamic analysis of subcritical high-temperature heat pump using low GWP refrigerants: a theoretical evaluation. Energy Convers. Manag. 268, 116034.

Urchueguía, J.F., Corberán, J.M., Gonzálvez, J., Díaz, J.M., 2004. Experimental characterization of a commercial-size scroll and reciprocating compressor working with R22 and propane (R290) as refrigerant. Ecobibrium J. AIRAH 23–25.

Uvsløkk, S., Schlemminger, C., Asphaug, S., 2017. Thermal insulation performance of reflective foils in floor cavities-Hot box measurements and calculations. Energy Procedia 132, 333–338.

van Soest, H.L., de Boer, H.S., Roelfsema, M., Den Elzen, M.G., Admiraal, A., van Vuuren, D.P., Hof, A.F., van den Berg, M., Harmsen, M.J.H.M., Gernaat, D.E.H.J., 2017. Early action on Paris Agreement allows for more time to change energy systems. Clim. Change 144, 165–179.

Van Vuuren, D.P., Meinshausen, M., Plattner, G.-K., Joos, F., Strassmann, K.M., Smith, S.J., Wigley, T.M.L., Raper, S.C.B., Riahi, K., De La Chesnaye, F., 2008. Temperature increase of 21st century mitigation scenarios. Proc. Natl. Acad. Sci. 105, 15258–15262.

Vignesh, G., Sanketh, A. V, Bellundagi, S.S., Kembhavi, S., Swamy, A.R.K., 2019. Solar powered air-cooling system for idle parked cars.

Viguié, V., Lemonsu, A., Hallegatte, S., Beaulant, A.L., Marchadier, C., Masson, V., Pigeon, G., Salagnac, J.L., 2020. Early adaptation to heat waves and future reduction of air-conditioning energy use in Paris. Environ. Res. Lett. 15.

Xu, X., Hwang, Y., Radermacher, R., 2013. Performance comparison of R410A and R32 in vapor injection cycles. Int. J. Refrig. 36, 892–903.

Zhou, G., Zhang, Y., Yang, Y., Wang, X., 2010. Numerical model for matching of coiled adiabatic capillary tubes in a split air conditioner using HCFC22 and HC290. Appl. Therm. Eng. 30, 1477–1487.